

The role of recovery forces in the deformation of linear polyethylene

D. G. FOTHERINGHAM, B. W. CHERRY

Department of Materials Engineering, Monash University, Clayton 3168, Victoria, Australia

In the light of the finding that the deformation of linear polyethylene is associated with the development of recoverable strain, a technique has been developed to determine the magnitude of the recovery forces. The difference between the applied force and the recovery force represents the effective force which acts on the anelastic processes and a consideration of the kinetics of deformation suggests that the anelastic process consists of the co-operative movement of a number of molecular segments. The extrapolated yield point appears to be associated with the effective force and has no particular structural significance, in that it corresponds merely to the point of maximum curvature in the relationship between effective stress and rate of deformation.

1. Introduction

1.1. Nature of the yield point

There are, in general terms, two distinct classes of theory which have been put forward to explain the time and temperature dependence of the yield point in polymers. In this paper the mechanisms associated with the two classes of theory will be termed "nucleation" controlled and "velocity" controlled.

"Nucleation controlled" mechanisms of yield have been put forward by, among others, Peterson [1], Bowden and Raha [2] and Young [3]. This mechanism describes the yield process as arising from the stress-activated thermal initiation of dislocations (or dislocation analogues [2]) and assumes that the Peierls stress is considerably less than that required for nucleation.

"Velocity controlled" mechanisms of yield have similarly been put forward by a number of workers including Robertson [4], Cherry and Holmes [5] and Bauwens-Crowet [6]. The proponents of these mechanisms do not concern themselves with the initiation of the deformation mechanisms involved, but consider that the yield point corresponds to the point where the stress-activated movements of the dislocations or vacancies give rise to a rate of deformation which

is equal to the impressed rate of deformation. The treatment is similar to that put forward originally by Eyring [7] to describe the viscosity of a fluid.

Both "velocity controlled" and "nucleation controlled" mechanisms give rise to expressions for the dependence of the yield stress on the strain rate which are precisely similar in form but which differ in the interpretation which is applied to the parameters involved.

It has been shown in an earlier paper [8] that the development of permanent plastic strain in linear polyethylene is a continuous function of the applied strain, showing no discontinuity at the extrapolated yield point. It may also be noted that the yield stress (defined by the appearance of slip bands) of amorphous polymers falls to zero as the temperature rises to the glass transition temperature of the polymer [9]. If, therefore, polyethylene is deformed at temperatures above its glass transition temperature and if the amorphous component of the material is responsible for at least a portion of the strain developed, then it seems likely that the initiation of plastic strain would play no part in determining the yield point of the material. It seems much more likely that the yield point is controlled by the kinetics of a process which occurs at strains both greater and less than the yield strain.

1.2. The kinetics of yield

The classical treatment of velocity controlled deformation describes the deformation in terms of "mobile units" (which may be dislocations, vacancies, molecular segments etc.) which move from one position of minimum local free energy to an adjacent position across an intervening activation energy barrier by means of stress-activated thermal diffusion [4–7]. Such a model will give rise, under conditions of high stress and low temperature to a linear plot of yield stress against the log of the strain rate.

This simple model has had to be modified to take account of a number of experimental observations. Bauwens-Crowet *et al.* [10] have accounted for the curvature of the line representing the relationship between the yield stress and the log of the strain rate for some glassy polymers by postulating that at high strain rates and low temperatures an additional but similar stress-activated process also plays a role in controlling the deformation.

The "activation volume" is defined as the product of the area swept out by the mobile unit in moving from one local free energy minimum to the next and the resolved component in the direction of the applied stress of the distance moved by the mobile unit. The interpretation of the magnitude of the activation volume has presented difficulties. Haward and Thackray [11] who found a range of values between 3.1 and 28 nm³, compared this with the volume of a molecular statistical link in solution, between 0.3 and 2 nm³ and concluded that the results seemed "very much in line with the basic concepts of the Eyring theory". Cherry and McGinley [12] reported a value for the activation volume in branched polyethylene of 29 nm³ and interpreted this as a dislocation of length 116 nm but failed to show that dislocations were the mobile units. Robertson [4], in order to reconcile the experimental values which he found for the activation volume of polycarbonate, was forced to introduce a stress concentration factor which was "about fifty".

The classical treatments of "velocity controlled" yield have all considered that the activation volumes for forward and backward movement of the mobile unit are the same. Nichols [13] has pointed out that this assumption is not necessarily justified in metals and there seems to be no reason for it to be justified in polymers either.

Classical treatments of velocity controlled yield have also considered that the local free energy minima between which mobile units may jump, although separated by activation energy barriers, are themselves of the same energy level and so no energy is stored in the system as a result of the movement of the mobile units. If the local free energy minimum to which a mobile unit jumps is at a higher energy level than its source, then on removal of the applied stress, thermal activation may allow the mobile unit to move back to its original position and the process may be described as anelastic rather than plastic. It should be noted that in a previous paper [8] it was suggested that the strain rate dependence of the stress required to bring about a given strain must be associated with anelastic rather than plastic processes and so it may be assumed that energy is stored in the material as a result of the motion of mobile units.

1.3. Asymmetry of activation volumes

The classical expression given by Eyring for the rate of flow in a liquid [14] can be written as

$$\dot{\epsilon} = K \exp(-Q/kT) [\exp(v\tau/2kT) - \exp(-v\tau/2kT)] \quad (1)$$

where $\dot{\epsilon}$ is the strain rate, Q the activation energy v the activation volume, τ the applied stress and K is a constant which includes the factors converting shear to linear strain. All the other symbols have their usual meaning.

If however the activation volume for forward movement of the mobile unit differs from that for backward movement, then Equation 1 must be modified and writing η for the ratio of backward activation volume to the forward activation volume the expression becomes

$$\dot{\epsilon} = K \exp(-Q/kT) [\exp(v'\tau/2kT) - (-\eta v'\tau/2kT)] \quad (2)$$

where v' now refers only to the forward activation volume. At high stresses and low temperatures Equation 2 reduces to

$$\dot{\epsilon} = K \exp(-Q/kT) \exp(v'\tau/2kT)$$

which is indistinguishable from the similar approximation for Equation 1. The existence of the term η does, however, make a considerable difference to the curvature of the relationship between the applied stress and the log of the strain

rate, in the region where the linear relationship between the two terms is not applicable.

1.4. Anelastic processes

As well as the possible asymmetry of the activation energy barrier, the relative heights of successive local potential energy minima must be considered. The recoverability of the process controlling the rate dependence of deformation has suggested that there is a successive increase in height of the local potential energy minima as deformation proceeds. An exactly equivalent representation of such a process is an activated rate process in which successive local free energy minima are all of the same energy but which operates in parallel with an elastic (not necessarily linear) process.

The Cherry and Holmes model of yield [5], later applied by Cherry and McGinley [12, 15], suggests that yield occurs when a critical strain value is achieved in the intercrystalline, or "amorphous", regions of the polymer. These regions deform in parallel with the crystalline lamellae, the latter controlling the time-dependent part of the stress according to the rate of propagation of dislocations within the lamellae.

Haward and Thackray [11] have used a model similar to that of Cherry and Holmes to describe the stress-strain curves of amorphous polymers up to large strain values, but instead of a linear elastic element they incorporated a Langevin spring to take account of the rubber-like origin of the elastic forces. In fact they found little improvement over the linear element at low strains.

In general any model of this type can be represented by a storage element S in parallel with an activated rate process (Fig. 1). The inclusion of a series element to allow for the finite instantaneous elastic modulus makes the argument more complete. Since the stress in S_1 is associated with the process of recovery, it may be termed the recovery stress σ_r . Hence if σ_a is the total stress which is applied to the system, the "effective" stress σ_e , which is that stress which actually brings about the activated rate process of plastic deformation, is given by

$$\sigma_e = \sigma_a - \sigma_r. \quad (3)$$

It is the effective stress which must be used in attempting to consider the kinetics of the rate-controlling deformation processes. When the applied stress equals the recovery stress, the

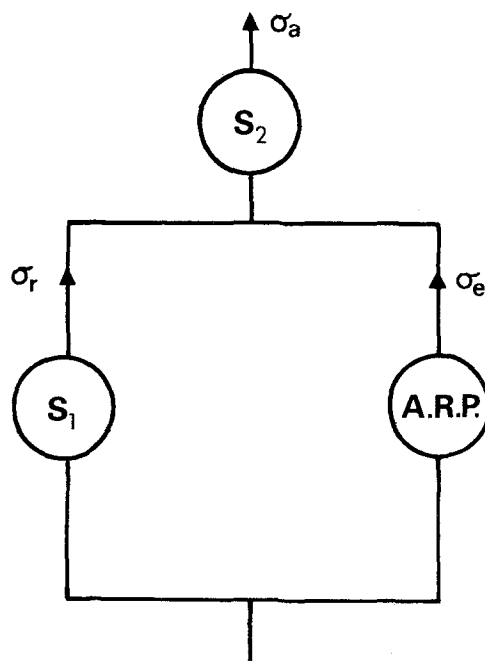


Figure 1

effective stress is zero and hence so is the strain rate. This forms the basis of the method for determining the recovery stress.

1.5. Determination of recovery stresses

By definition the recovery stress is analogous to the internal stress in a deformed metal [16] and may be determined by techniques which have been developed for internal stress determinations [17]. An approach which can be performed with relatively unsophisticated testing equipment is the stress-transient dip test. This involves a rapid unloading step from the stress-strain condition to be examined to a new test stress σ_T . The strain is then held constant and the stress monitored as a function of time. As before if $\sigma_T = \sigma_r$ a zero strain rate will result and the stress will remain constant. If $\sigma_T > \sigma_r$ then σ_e will be positive and a positive viscous flow (relaxation) will result so that initially σ_T will decrease. If $\sigma_T < \sigma_r$ then σ_e will be negative and an increase in stress will follow. Such a test sequence was tried for HDPE and the result is shown in Fig. 2. It will be noted that there is fairly broad band over which the initial response shows neither relaxation nor recovery, presumably because of the limitations of the load measurement system. This will be discussed further in Section 2.2. The recovery stress has been interpreted as the centre of this band.

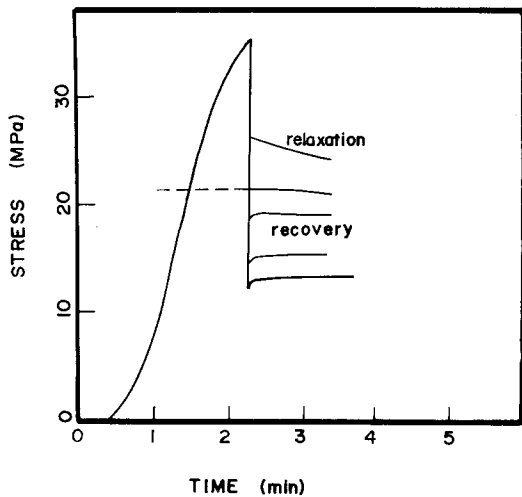


Figure 2 The stress-transient dip test.

It will also be seen that an initial recovery response may be followed by a relaxation at longer times. This is an indication that the structural elements giving rise to the recovery stress may themselves relax. A similar result was found for metals at high temperature (Solomon *et al.* [17]) and was used to demonstrate the need for only one unloading step in the test sequence. It is therefore important that the initial response to the stress transient should be recorded and for this reason only single unloading steps were used in this work.

2. Experimental

2.1. Materials and apparatus

The material used was a linear polyethylene of density 961 kg m^{-3} and is described in detail in an earlier publication [8]. Recovery stress measurements were made using plane strain compression at constant cross-head speed. Two specimen configurations were employed. The first, described in the earlier work [8], was used for comparison with the results of strain recovery tests which used the same conditions. However, it was found in practice that the specimen strain rate could vary by as much as a factor of 10 at constant cross-head speed, and this was unsatisfactory for meaningful measurements of recovery stress. The variation is a result of deflections in the testing system which can be reduced by reducing the load. A second system was therefore employed with dimensions:

$$\begin{aligned} \text{die breadth } b &= 6.35 \pm 0.01 \text{ mm} \\ &(0.2500 \pm 0.0005 \text{ in}) \end{aligned}$$

$$\begin{aligned} \text{specimen width } w &= 25.4 \pm 0.05 \text{ mm} \\ &(1.000 \pm 0.002 \text{ in}) \\ \text{specimen thickness } t &= 2.46 \pm 0.05 \text{ mm} \\ &(0.097 \pm 0.002 \text{ in}) \end{aligned}$$

These values give b/t and w/b ratios within the range recommended by Williams and Ford [18]. The change of strain rate was thereby reduced to a factor of 2.4. While this is not entirely satisfactory it is difficult to reduce this figure further as the testing system stiffness decreases with load.

2.2. The recovery stress during deformation

The recovery stress was determined by means of the stress-transient dip tests using an Instron TTD Testing Machine. The maximum and test loads respectively are set as the upper and lower limits on the load cycling cams and the cycling controls switched to "cycle and stop". If the two cross-head speeds are then selected as described below the test will run automatically.

A number of modifications were required to the Instron Testing Machine to allow the rapid unloading step to be controlled. These involved:

(i) Short circuiting the cross-head error integrator device – this means that larger errors in the cross-head position may occur but the response time to a transient is improved markedly.

(ii) Wire links to activate the "traverse" clutch when the cross-head is moving down. The required links are between terminals 1 and 8 and between 11 and 13 on the push-button cross-head speed controller. It should be noted that these may be live (110 V a.c.) and so due care must be taken. A consequence of the links is to cause the traverse switch to make the cross-head move down regardless of the direction selected. The outcome of this modification is that the "up" speed may be selected on the push-buttons while the "down" speed is that set for traverse operation. These correspond to the test and unloading speeds respectively.

While the speed of response of a screw-driven machine is not as fast as that which can be obtained using a servo-hydraulic machine, the plane strain testing configuration means that very small cross-head movements are required to effect the desired change in stress. This helps to counteract the slower response and it was found in practice that using a high speed Leeds and Northrup chart recorder and an unloading rate of 50.8 mm min^{-1} (2.0 in min^{-1}) the time required for the

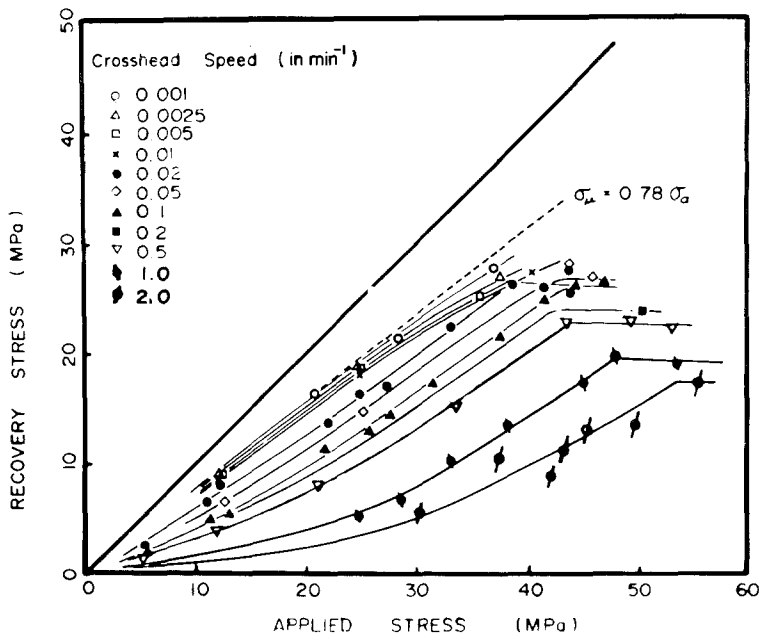


Figure 3 The recovery stress as a function of applied stress, determined at various cross-head speeds.

machine to reach equilibrium for a typical transient was less than 0.1 sec. This value was determined with no specimen between the dies so that material transients could be eliminated. When a specimen is inserted the cross-head travel will be greater because of the lower stiffness of the system. Since in the region of testing the machine stiffness and specimen stiffness are comparable, the time to reach equilibrium should be approximately twice that without a specimen. In practice an overshoot of duration less than 0.25 sec in the load reading was commonly observed, and hence all readings were taken at times longer than this.

The inherent mechanical lag in the unloading step led to considerable overshoot of the pre-set load value which was rather troublesome at very low loading rates where a small stress transient was desired. It was found necessary to decrease the unloading rate under such conditions and preliminary tests showed that the values of recovery stress were within experimental error providing an unloading rate at least five times the loading rate was used.

At high loading rates $> 12.7 \text{ mm min}^{-1}$ ($> 0.5 \text{ in min}^{-1}$) this condition will obviously not be fulfilled since the highest unloading speed which could be controlled was 50.8 mm min^{-1} (2.0 in. min^{-1}). For this reason the experimental scatter is larger at high cross-head speeds. It should be noted however that errors of this type should

lead to high rather than low values for the recovery stress.

The recovery stress was first determined as a function of applied stress for each cross-head speed and these results are shown in Fig. 3. Subsequently a single stress-strain curve was obtained for each cross-head speed and these results (Fig. 4) were used to calculate the recovery stress as a function of strain. These latter results are shown in Fig. 5. Because many of the points lie close together in the low strain region the results in Fig. 5 are presented for only four cross-head speeds.

3. Results

3.1. The recovery stress as a function of strain

It is clearly evident that up to the strain corresponding to the EYP [8] the recovery stress is a linear function of strain at a given cross-head speed (Fig. 5). After the EYP the rate of increase falls off until a value of strain of approximately 0.3. Above this value there is no consistent trend in results and, in fact, two of the curves actually cross. While much of this behaviour may be explicable in terms of changes in specimen strain rate during a test, the region beyond a strain of 0.3 is not important to this work and will therefore be ignored.

The actual fall in recovery stress from a linear

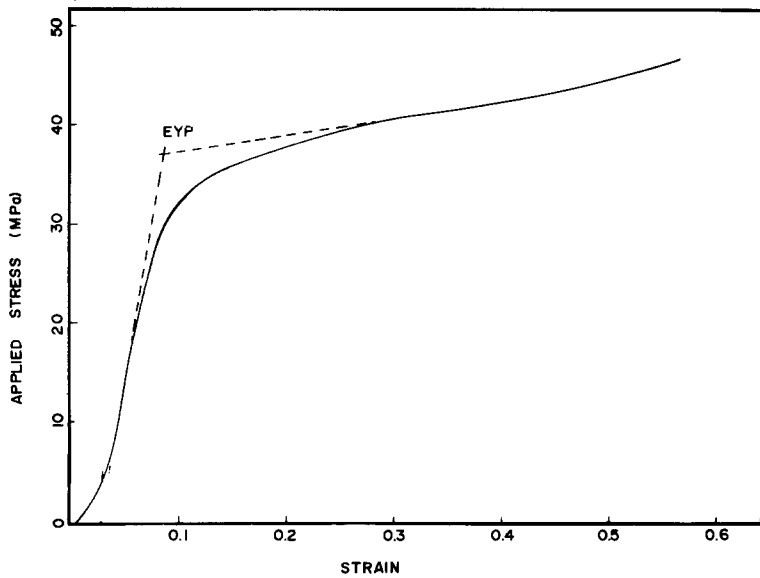


Figure 4 The applied stress as a function of strain.

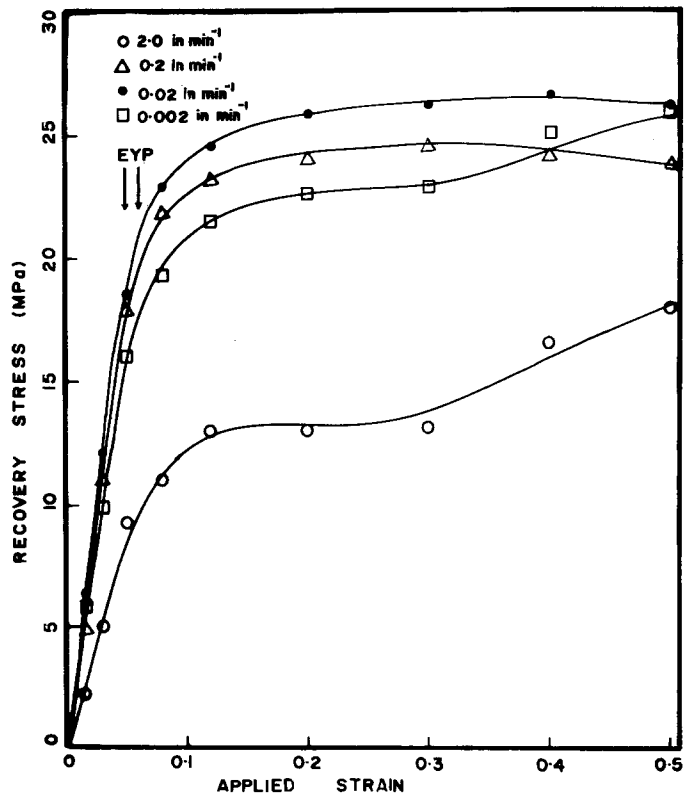


Figure 5 The recovery stress as a function of strain determined at four cross-head speeds.

relation with strain does not become significant until the strain is well beyond that at the EYP, whereas the applied stress has deviated considerably from linearity at this point (Fig. 4). Thus the structural component giving rise to the recovery stress cannot be responsible for the observed drop in stress in the range of the EYP. On the other hand, the recovery stress does level off significantly

at higher strain values and can therefore be expected to influence the shape of the stress-strain curve in this range ($\epsilon > 0.1$).

3.2. The recovery stress as a function of cross-head speed

In Fig. 6, the recovery stress at constant strain is plotted as a function of cross-head speed. There is

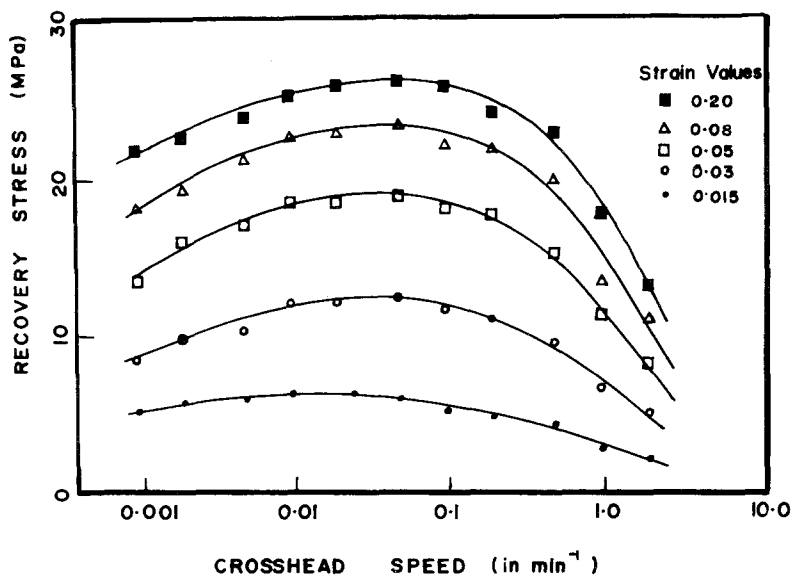


Figure 6 The recovery stress at constant strain as a function of cross-head speed.

a dramatic fall as the cross-head speed increases above 5 mm min^{-1} (0.2 in min^{-1}) and a more uniform decrease as it falls below 0.25 mm min^{-1} (0.01 in min^{-1}). In an attempt to determine whether the fall-off in recovery stress at the highest cross-head speeds could be due to adiabatic heating, measurements of the temperature rise during deformation were made by inserting a thermocouple into the specimen. Since the observed temperature rise was less than 0.5°C it was concluded that adiabatic heating was unlikely to be the cause of the fall-off. As noted in Section 2.2, the effect at high cross-head speed where the unloading rate is similar to the loading rate would be to increase the time for which the specimen is at high stress. This would cause the recovery stress value to tend towards that for a lower loading rate and hence would lead to abnormally high values for the recovery stress (Fig. 3). This, therefore, cannot explain the observed drop in the measured values for the recovery stress.

It can be seen from Fig. 3 that there is an apparent upper limit to the value of σ_r at around $0.78 \sigma_a$, even at very low strain rates, and it is suggested that this limit of σ_r at low speeds may be due to a time-dependent relaxation of the stress in the part of the structure causing the recovery stress. Such a relaxation, if it occurs, must be slow compared with the rate of relaxation of the remaining effective stress, and could therefore account for the relaxation response at long times

in the stress-transient dip test when an initial recovery response was observed.

The rapid fall in recovery stress at high cross-head speed may well account for the decrease in slope of the applied stress against cross-head speed curves in this range [8]. Thus the levelling off of the yield stress at the lowest temperatures and highest cross-head speeds could arise from the reduction in the contribution of the recovery stress to the total applied stress in these conditions.

A point which may be noted is that the measured recovery stress is a maximum for a cross-head speed of 0.5 mm min^{-1} (0.02 in min^{-1}). This cross-head speed also corresponds ([8], Fig. 1) to the maximum value of the recoverable strain. The general trends of decreasing recoverability ([8], Fig. 1) and recovery stress (Fig. 6) at higher strain rates and the less rapid change at lower strain rates also correlate, although the relative magnitudes differ somewhat for the cross-head speeds of 0.05 mm min^{-1} ($0.002 \text{ in min}^{-1}$) and 5 mm min^{-1} (0.2 in min^{-1}). This may be due to the difference in specimen dimensions since recovery stress determinations on larger specimens show that the order is reversed. Such a difference is quite reasonable when it is considered that the strain rate up to EYP is approximately four times higher for the small specimen than the large one.

Hence it can be seen that there is a similarity between the recovery stress and recoverable strain over the range tested. However, the different

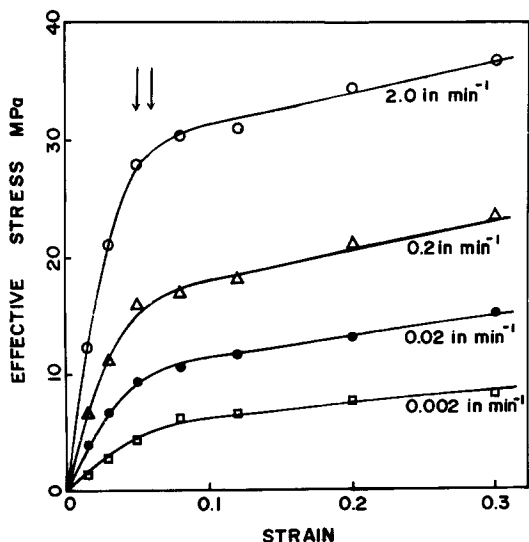


Figure 7 The effective stress as a function of strain determined at various cross-head speeds.

specimen geometries and other sources of error mean that quantitative comparisons are pointless.

3.3. The effective stress as a function of strain

The division of the applied stress into recovery stress and effective stress was suggested as a means of eliminating the effect of processes which store elastic energy during deformation, and hence sustain some of the applied stress. The remainder of the stress should be borne by viscous processes and hence should be amenable to a conventional treatment of thermally activated flow.

In Fig. 5 it can be seen that the recovery stress does not deviate significantly from linearity until a strain too large to account for the EYP. Therefore it is to be expected that the effective stress must be the cause of the yield behaviour. To confirm this, effective stress has been plotted against strain for four cross-head speeds in Fig. 7. The rapid curvature in the region of the EYP confirms that the effective stress is the part of the applied stress responsible for the change in slope of the stress-strain curve at this point.

3.4. The effective stress as a function of strain rate

The effective stress is plotted against log specimen strain rate for a number of values of strain in Fig. 8. While there is considerable scatter in the results, largely due to errors in the measurement of the recovery stress, it can be seen from Fig. 9 that the curves may be shifted horizontally to form a master curve without increasing the scatter significantly. The fact that a master curve may be formed without any vertical shift implies that the effects of other processes, which sustain part of the applied stress but which are not time-dependent on the scale of the experiment, have been eliminated. Thus the effective stress may be considered to be the stress acting on the viscous deformation mechanism.

The shift along the strain rate scale required to effect a super-position of the curves may be interpreted as a result of the finite elastic modulus of the polymer. When the effective stress is less

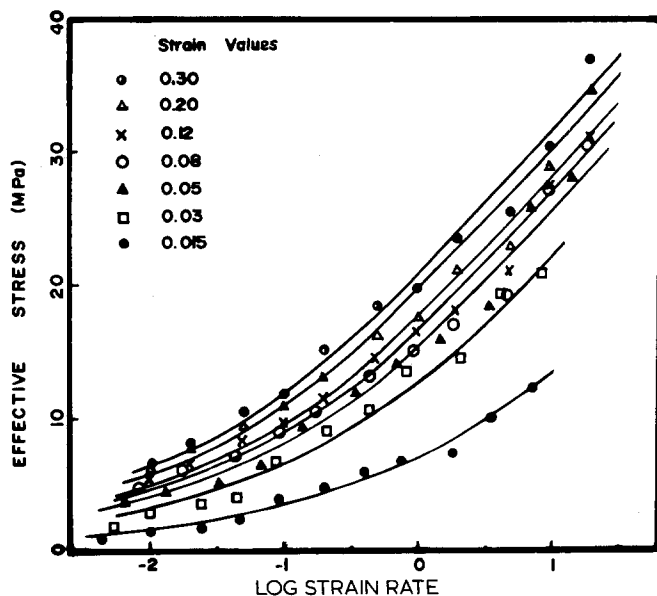


Figure 8 The effective stress at constant strain as a function of strain rate.

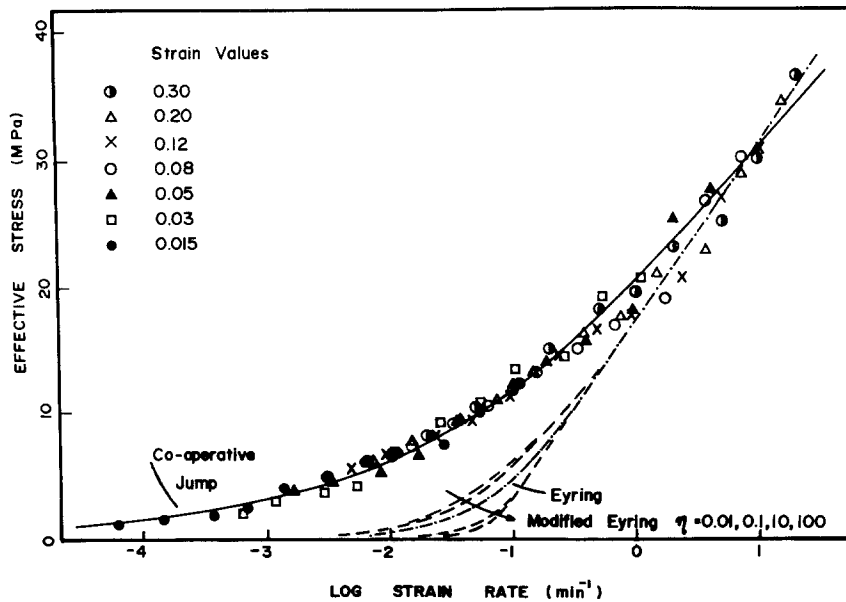


Figure 9 The master curve of effective stress as a function of strain rate. The broken lines represent the predictions of the simple Eyring theory modified for different ratios of forwards and backwards activation volume. The solid line represents the best fit for a co-operative jump theory with equal forwards and backwards activation volume.

than that required to make the viscous element deform at the applied strain rate, the remaining deformation will be elastic. Hence the stress-strain curve represents a progressive transition from elastic to viscous flow, and the EYP is indicative of the transition. The fact that the EYP occurs at almost constant strain at the test temperature (27°C) indicates that the change from elastic to viscous flow is strain dependent,

thus justifying the shifting of the curves at constant strain.

At the largest strain value (0.3), the viscous strain rate should be almost exactly equal to the applied strain rate, and hence this curve is used as a reference and the other curves shifted to it. The value of the shift factor $S(\epsilon)$ required to superimpose the curve at a strain ϵ onto the reference curve is plotted as a function of strain in Fig. 10.

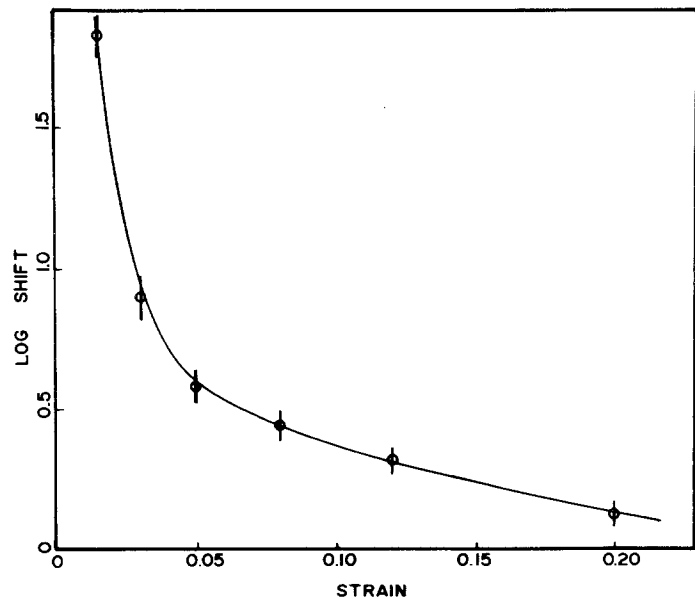


Figure 10 The shift factor as a function of strain.

The expected trend of an initial rapid change followed by a levelling off at high strain can be observed, tending to confirm the transition from elastic to viscous flow as the strain increases.

4. Discussion

4.1. Activated rate process theory

The high stress approximation to the Eyring equation (Equation 1) predicts a linear relationship between effective stress and log strain rate if a single mechanism is operating. This is obviously not the case for the master curve of Fig. 9 and in order to obtain agreement a continuous change of activation volume would be necessary, which seems unlikely.

The complete form of the Eyring equation predicts continuous curvature at low stress tending towards a linear relation at high stress. Such a curve can be obtained by fitting a straight line to the high stress data in Fig. 9 and the full curve which results is superimposed on the experimental points. Obviously the fit is very poor except in the linear range. In an attempt to improve the fit, the Eyring equation modified to allow for a difference between the forward and backward activation volumes [13] was also used. These results are also shown in Fig. 9 and although it can be seen that variations of η change the curvature of the line relating effective stress to log (cross-head speed), there is no reasonable value of η which can bring the actual and theoretical curves into coincidence.

From the trends observed in Fig. 9 it may be suggested that a modified Eyring equation with $\eta = 0$ would give the best fit. Such a theoretical curve would differ only fractionally from that for $\eta = 0.01$ and would still lie a long way away from the experimental points. In fact it is difficult to imagine a physical situation in which the ratio of the activation volumes is much less than unity.

4.2. A model based on co-operative jumps

It has frequently been suggested (e.g. [11]) that in a solid polymer the independent motion of chain segments would be most unlikely and that a co-operative motion would be necessary to permit significant flow. Such a concept was invoked to explain the high values of activation volume determined from yield stress data compared with the expected segmental volume. However, the conventional approach has been to treat the entire process as a whole, rather than to examine the

individual segment motions as separate events. It is the latter approach which will be investigated here.

Consider the thermally activated transition of a deformation entity across an energy barrier of height Q under the action of an effective shear stress τ_e . Now the recovery stress has been chosen to correspond to the zero strain rate condition, i.e. when the applied stress τ_a equals the corresponding recovery stress τ_r the strain rate will be zero and hence the energy states on either side of the barrier will be equivalent. Thus the probability of the entity being on either side of the barrier will be the same.

If an extra stress τ_e is applied then the transient response may be calculated using the model of Eyring [14]. The net rate of transition from Site 1 to Site 2 will then be

$$R = R_0 \exp(-Q/kT) \sinh\left(\frac{v^* \tau_e}{2kT}\right) \quad (4)$$

where v^* is the activation volume and R_0 is a slowly varying function of temperature which includes the translation partition function and a transmission coefficient.

Hence the average probability per unit time of an entity moving from Site 1 to Site 2 will be

$$p_1 = p_0 \exp(-Q/kT) \sinh\left(\frac{v^* \tau_e}{2kT}\right) \quad (5)$$

where p_0 is a constant which includes R_0 .

If a successful co-operative event involves the simultaneous occurrence of n such transitions, then the probability p_n of the co-operative process will be

$$p_n = \left[p_0 \exp\left(-\frac{nQ}{kT}\right) \sinh^n\left(\frac{v^* \tau_e}{2kT}\right) \right]^n \quad (6)$$

If the macroscopic strain caused by one such co-operative event is ϵ_0 then the strain rate $\dot{\epsilon}$ will be given by

$$\dot{\epsilon} = K_0 \exp\left(-\frac{nQ}{kT}\right) \sinh^n\left(\frac{v^* \tau_e}{2kT}\right) \quad (7)$$

where K_0 is a constant dependent of p_0 , ϵ_0 and n .

If the effective shear stress τ_e is assumed proportional to the effective applied stress σ_e then Equation 7 may be rewritten

$$\dot{\epsilon} = K_0 \exp\left(-\frac{nQ}{kT}\right) \sinh^n\left(\frac{v^* \sigma_e}{2kT}\right) \quad (8)$$

It will be noted that at high stress a linear relation between σ_e and \log (strain rate) will be obtained, as with the Eyring treatment, but that in the present case the measured value of $v^{*'} will be reduced by a factor n from the equivalent term in the Eyring equation and the approximation will not be valid until a much higher value of stress. Additionally any calculated value for the activation enthalpy Q will be reduced by a factor n .$

4.3. Comparison with experimental results

All the effective stress data in this work have been collected at a single temperature and hence Equation 8 may be simplified to

$$\dot{\epsilon} = K_T \sinh^n \left(\frac{v^{*'} \sigma_e}{2kT} \right) \quad (9)$$

where K_T now includes the temperature dependent term $\exp(-nQ/KT)$

Since there are three parameters involved it is most convenient to use a computer curve-fitting program to optimize their values. A least squares minimization program utilizing Marquardt's method was used. Although in the type of test used the strain rate should be considered the independent variable, a better fit is obtained by making the stress the independent variable since with the strain rate on a logarithmic scale the percentage error rather than absolute error is minimized, and this is consistent with the experimental errors.

The master curve fitted to the points in Fig. 9 was obtained by this method and the resulting values for the parameters are; $n = 3.1$, $v^{*'} = 0.570 \text{ nm}^3$, $K_T = 0.127$

It can be seen that the fit of the experimental points to the derived curve is very good, and it is believed that this adds weight to the concept that it is a co-operative activated rate process which controls the rate dependence of the deformation in linear polyethylene.

4.4. The physical basis for a co-operative jump process

It may be of interest to speculate on the nature of the co-operative activated rate process which is describable by the parameters derived in Section 4.3. Whilst no concrete evidence can be put forward to validate the model proposed below it is believed that it is consistent with the results published above and in a previous paper [8].

Young, Bowden and Rider [19] have suggested that interlamellar slip contributes largely to the recoverable deformation in linear polyethylene. Andrews [20] has shown that the effects of crystallinity and irradiation on the stress-strain curves for various polyethylenes could be described by a model in which the extrapolated yield point was controlled by the average area of contact between adjacent lamellae. Although he interpreted the extrapolated yield point as a transition from recoverable slip, an interpretation which cannot be given to the results detailed above, the concept of mechanical interaction of the chain loops at the lamellae contact surfaces might be applicable to the time dependence observed for interlamellar slip.

If the anelastic deformation process involves slipping of chain-folded lamellar surfaces over one another then we may estimate the activation volume v^* for this mechanism by considering a simple model for the chain-folded surface. While it is now widely believed that the fold surfaces in bulk spherulitic polyethylene are composed of irregular folds (Mandelkern [21]), it is difficult to obtain a value of v^* in this case and so it is preferable to assume a regular fold surface and then consider the effect of a relaxation of this assumption.

A model for the fold surface of a flat lamella of polyethylene is given by Reneker and Geil [22]. This is shown schematically in Fig. 11. If a second lamellar surface is in contact with that shown, then two stable positions for a loop in this second surface would be those marked A and B. If the lamellae are sheared with respect to one another then it is to be expected that such a shear would occur by displacements of the loops between such positions. The linear displacement between A and B is

$$d_{AB} = \sqrt{(a^2 + b^2)}$$

where a, b are the crystal parameters.

Now the activation volume v^* is the product of d_{AB} with the average area sheared per loop movement. This area may be evaluated by considering the area enclosed by dotted lines in Fig. 11. The area of this region is $4ab$, and there are four loops so that the average area sheared per loop will be ab . Hence v^* is

$$v^* = ab \sqrt{(a^2 + b^2)} \quad (10)$$

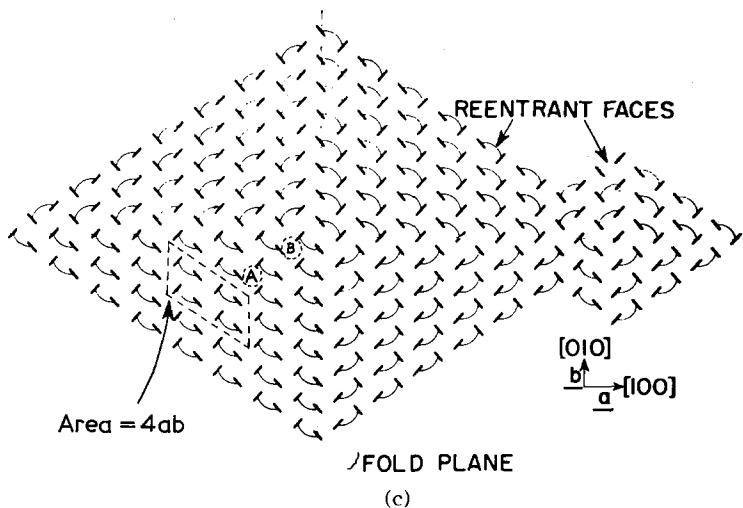


Figure 11 Projection of a regular fold surface for a polyethylene crystal (after Reneker and Geil [22]) showing the stable positions for a loop in an adjacent surface.

which, substituting the values for the crystal parameters in HDPE gives $v^* = 0.326 \text{ nm}^3$.

The value of v^* from the curve-fitting program is 0.570 mm^3 . In order to calculate v^* from v^* it is necessary to know the relationship between the shear stress, which activates the deformation process, and the applied compressive stress. The work of Bowden and Jukes [23] shows that the yield stress in pure shear τ_y may be calculated from the yield stress in plane strain compression σ_y by assuming a modified von Mises criterion. They derived the expression

$$\tau_y = (\sigma_y/2)(1 - \mu)$$

where μ is a constant which was determined for HDPE by Rabinowitz *et al.* [24] as 0.034. Hence it will be assumed that $\tau_e \approx 0.48 \sigma_e$ and hence that v^* is approximately 1.18 mm^3 or about three times the theoretical prediction.

There are, however, two effects which would tend to lead to such a discrepancy. The first is the stress concentration due to the effect of regions of lamellae which are not in mechanical contact and the second is the likelihood of an irregular fold surface.

Using the model proposed by Andrews [20] certain regions of the lamellar surface will not be in mechanical contact with adjacent surfaces, and therefore will be free to slide once the regions in contact permit. This would lead to a stress concentration on the contact regions equal to the ratio (total lamellar area:contact area). For a density of 961 kg mm^{-3} the crystallinity will be approximately 0.7 and then the "lamellarity" will

be ~ 0.8 (Andrews [20]). Thus the fraction of the lamellar surfaces in contact is $L^2 = 0.64$ and the resulting stress concentration factor is about 1.5. Therefore, although the measured activation volume will be larger than the true value by this factor, this effect is not by itself sufficient to account for the measured discrepancy.

The further factor of approximately two may be explained if the fold surface is irregular and the average number of folds in contact per unit area of lamella is less than that which would be predicted on the basis of regular folding. This will increase the activation volume since both the average linear movement per fold and the average area sheared per fold will increase.

If the number of interacting folds per unit area in a regular interlamellar surface is f_r and this is reduced to f_i in an irregular surface, then the activation volume, calculated by the method which led to Equation 10, should increase by a factor

$$\frac{v_i^*}{v_r^*} = \left(\frac{f_r}{f_i}\right)^{1/2} \left(\frac{f_r}{f_i}\right) = \left(\frac{f_r}{f_i}\right)^{3/2}$$

Utilizing the experimental and theoretical values for v^* and including the effect of stress concentration leads to a ratio $f_i/f_r = 0.56$, which would indicate a reasonably irregular fold surface.

It should be noted, however, that the experimental errors in measuring recovery stress together with the insensitivity of the theoretical curve to changes in v^* and n means that a reasonable fit could be obtained even with the value of v^*

increased by a factor of two. Thus no conclusive evidence could be inferred as to the nature of the fold surfaces from the above observations.

The value $n = 3.1$ indicates that about three folds on average would need to shift co-operatively to allow the deformation to proceed, and this seems reasonable in an irregular structure where the loops are comparatively free to move. A higher value of n would be expected in a regular fold surface since the loops would be more tightly bound.

5. Conclusions

5.1. Deformation of linear polyethylene

In this paper and a previous one [8] it has been shown that:

(a) There is an irrecoverable strain response to the application of any stress, however small.

(b) The rate dependence of the deformation is associated with recoverable strains.

(c) The difference between the applied force and the recovery force represents the effective force which acts to bring about the anelastic deformation.

(d) When the effective force rather than the applied force is considered, the anelastic deformation may be described as a co-operative activated rate process.

Young, Bowden, Ritchie and Rider [19] have suggested that $\langle 001 \rangle$ slip processes in the crystalline region of the polymer account for the permanent deformation, whilst interlamellar slip contributes largely to the recoverable deformation. If the fundamental rate process associated with $\langle 001 \rangle$ slip is simply the movement of a length of dislocation line through a distance of one Burgers vector and if the length of the dislocation line involved is about one unit cell, then the activation volume will be about 0.05 nm^3 hence the rate of the $\langle 001 \rangle$ slip will be much less sensitive to stress than that of the interlamellar slip. Under these circumstances the model proposed by Young *et al.* [19] is consistent with the observations (a–d) above. It also seems likely that intralamellar slip may bring about the relaxation of the recovery forces. This model differs in detail from one previously proposed [5] but seems more in accord with the facts which are now known.

5.2. Application to other polymers

The concepts of recovery stress and of a co-operative jump process are likely to be

applicable to deformation of other polymers. For example, Uhlmann and Park [25] have established that virtually all of the deformation in amorphous polycarbonate is recoverable on heating, so that there must be a considerable stored energy during deformation. Hence the use of the Eyring theory to explain the yield data must be highly questionable, particularly if the yield strain is not constant as has been shown for PMMA by Rusch and Beck [26].

The co-operative jump model has been used to explain some of the existing yield data for PMMA and PVC by the authors [27], although it is obvious that the approach requires knowledge of the recovery stress values which have not been measured for these polymers.

Acknowledgements

One of us (DGF) wishes to acknowledge the receipt of an APRA scholarship during the tenure of which this work was carried out. Both authors wish to thank the anonymous referee whose wish to see the authors comments on the values of the parameters derived from Fig. 9 led us to include Section 4.4. in this paper.

References

1. J. M. PETERSON, *J. App. Phys.* 37 (1966) 4047.
2. P. B. BOWDEN and S. RAHA, *Phil. Mag.* 29 (1974) 149.
3. R. J. YOUNG, *ibid* 30 (1974), 85.
4. R. E. ROBERTSON, *J. Appl. Polymer. Sci.* 7 (1963) 443.
5. B. W. CHERRY and C. M. HOLMES, *J. Phys. D* 2 (1969) 821.
6. C. BAUWENS-CROWET, *J. Mater. Sci.* 8 (1973) 968.
7. H. EYRING, *J. Chem. Phys.* 4 (1936) 283.
8. D. G. FOTHERINGHAM and B. W. CHERRY, *J. Mater. Sci.* (in press).
9. I. M. WARD, "The Mechanical Properties of Solid Polymer", (Wiley, London 1971) p. 316.
10. C. BAUWENS-CROWET, J. C. BAUWENS and G. HOMES, *J. Polym. Sci. A-2*, 7 (1969) 735.
11. R. N. HAWARD and G. THACKRAY, *Proc. Roy. Soc. A302* (1968) 453.
12. B. W. CHERRY and P. L. MCGINLEY, *Appl. Polymer Symp.* 17 (1971) 59.
13. F. A. NICHOLS, *Mater. Sci. and Engineering* 8 (1971) 108.
14. S. GLASSTONE, K. J. LAIDLER and H. EYRING, "The theory of rate process". (McGraw-Hill, New York 1941) p. 483.
15. B. W. CHERRY and P. L. MCGINLEY, *J. Macromol. Sci-Chem.* A6 (1972) 811.
16. J. J. JONES, *Acta Met.* 17 (1969) 397.
17. A. A. SOLOMON, C. N. AHQUIST and W. D. NIX, *Scripta Met.* 4 (1970) 231.

18. J. G. WILLIAMS and H. FORD, *J. Mech. Eng. Sci.* **6** (1964) 405.
19. R. J. YOUNG, P. B. BOWDEN, J. M. RITCHIE and J. G. RIDER, *J. Mater. Sci.* **8** (1973) 23.
20. E. H. ANDREWS, *Pure Appl. Chem.* **31** (1972) 91.
21. L. MANDELKERN, "Crystallization of Polymers", (McGraw-Hill, New York 1967).
22. D. H. RENEKER and P. H. GEIL, *J. Appl. Phys.* **31** (1960) 1916.
23. P. B. BOWDEN and J. A. JUKES, *J. Mater. Sci.* **7** (1972) 52.
24. S. RABINOWITZ, I. M. WARD and J. S. C. PARRY, *J. Mater. Sci.* **5** (1970) 29.
25. D. R. UHLMANN and J. B. PARK, *J. Appl. Phys.* **42** (1971) 3800.
26. K. C. RUSCH and R. H. BECK, *J. Macromol. Sci. Phys.* **B3** (1969) 365.
27. D. G. FOTHERINGHAM and B. W. CHERRY, *J. Mater. Sci.* **11** (1976) 1368.

Received 27 June and accepted 16 September 1977.